



## Vegetation Discrimination and Change Analysis Using Multi-temporal IRS-1C LISS III Imagery

Rubina Parveen<sup>1\*</sup>, Subhash Kulkarni<sup>2</sup> and VD Mytri<sup>3</sup>

<sup>1</sup>Research Scholar, VTU, Belgavi, Karnataka, India

<sup>2</sup>PESIT, Bengaluru (South Campus), Bengaluru, India

<sup>3</sup>AJET, Kalaburgi, Karnataka, India

\*Corresponding Author: Rubina Parveen, Research Scholar, VTU, Belgavi, Karnataka, India.

Received: January 23, 2019; Published: March 18, 2019

### Abstract

An IRS-1C LISS III image consists of numerous regions with hierarchical land cover. In this paper, Firstly, an attempt has been made for vegetation extraction and its discrimination into various classes. Geometrically co-registered multi-temporal IRS-1C LISS III satellite imagery were used for analysis. Secondly, processed Multi-temporal images were subjected for change analysis. The proposed algorithm sequentially performs pre-processing, image segmentation and classification. Study image was pre-processed by Partial-Differential Equation (PDE) based enhancement technique, followed by multiphase level set segmentation. Geometric properties were estimated for the evolving features using this curve propagation algorithm. Multiphase level set segmentation functions was employed to extract a set of regions of the evolved features and their set of boundaries. Vegetation features were separated by Normalized vegetation index (NDVI). Further, the vegetation patterns were classified hierarchically into discriminative classes. Chronological changes were detected in each class. Quantitative and qualitative analysis has been done. The quantitative assessment was presented by calculating overall accuracy of the algorithm and Kappa coefficients. The proposed algorithm was an automated process of vegetation discrimination and interpretation. It can be flexibly applied to geo graphically different areas.

**Keywords:** Vegetation; Multi-temporal; Segmentation; Algorithm

### Abbreviations

Indian Remote Sensing-1C Linear Integrated Self Scanning Sensor; PDE: Partial Differential Equation; NDVI: Normalized Difference Vegetation Index; GIS: Global Information System.

### Introduction

LAND-USE monitoring and management plays an important role in development of a country [1]. Monitoring the status of the natural resources, spatial-temporal change detection and land cover future prediction can be done by analysis of satellite imagery [2]. The task of land-use classification faces number of challenges due to presences of noises, time of acquisition [1] and due to spatial/spectral variations. Temporal changes generally change the land cover features [3]. Geometrically registered Multispectral digital image data set i.e. Indian Remote Sensing-1C Linear Integrated Self Scanning Sensor (IRS-1C LISS III) image was used to identify and analyze dynamics of land use. Spectral reflectance characteristics are dependent upon shape, pattern and color. These

geo physical features are prerequisite for interpreting distinctive land cover features in satellite image [4]. Visual analysis of the images has been done to identify broad type and number of classes for classification. Six major classes have been identified, namely water bodies, vegetation, bare land, harvested lands and built-up areas, in the study image. The study image was preprocessed by PDE-based nonlinear diffusion filters for image de-noising by employing famous total variation Model (TVM) [5]. Easy and fast intensity-based histogram equalization method [6], was used for enhancing visual clarity. Land cover types and relative hierarchical Structure [7] is difficult to extract [8] with low spatial resolution images. The level set multiphase image segmentation uses an active curve objective functional with two terms: an original term which evaluates the deviation of the mapped image data within each segmentation region and a classic length regularization term for smooth region Boundaries [9]. GLCM (Gray Level Co-occurrence Matrix) can provide important insight into the subsurface through attribute analysis [10]. Spectral indices i.e. NDVI (Normalized Dif-

ference Vegetation Index) has been employed due to superior and reliable vegetation feature extraction approach [11]. The spatial relationships of pixels are calculated by Euclidean distance, for pixel-based statistical classification [12]. The visual assessment of an images [13] is an vital factor for evaluating the effectiveness of this algorithm. Further, the spatio-temporal change detection analysis was carried out, that includes the integration of GIS and remote sensing methods [14]. Multi-temporal imagery was analyzed to extract phenological changes in the vegetation. MATLAB (2010a) and ERDAS IMAGINE 9.1simulation software were used because of high degree of flexibility. Preprocessing, segmentation and classification computation is done using the tools supported by MATLAB.

### Research Objectives

Accuracy of proposed algorithm was tested by extracting vegetation patterns. Multi-temporal image difference technique was executed to calculate occupancy of vegetation area. The research objectives were:

- To study and develop the algorithm for extracting vegetation and discriminate vegetation patterns.
- To study and estimate the area under different vegetation patterns.
- Accuracy estimation.
- To calculate the change in vegetation patterns of multi-temporal imagery.

### Study area and data set

The study was done using LISS III imagery of different seasons. A part of Yadgir District area, of Karnataka state, India, which was highly heterogeneous Study area [15], was taken for the study. The Yadgir area taken for the study was mainly covered with water body, irrigated land, rain fed land and sparse vegetation.

### Earth observation

The study frame is between the longitude 16 26 49.04||N to and latitude 76 50 02.96|| E. The proposed algorithm was tested on subsets frames of an IRS-1C LISS III remote sensing image data-set acquired on 20th October 2006 and 11th April 2006 with a spatial resolution 23.5mts, provided by Karnataka State Remote Sensing Centre, Regional Office Gulbarga, Karnataka state, India. An image pixel covers an area of approximate. 552.2 sq. m or 5.52 sq.km of land cover. The image frame is approximately 7067 pixels long and 7055 pixels wide. The figure 1 shows the area of analysis.

### Multispectral (MS) Images

The LISS-III is working in MS (multi-spectral) camera operates in four different spectral bands [16]. Four bands are: 1<sup>st</sup> band is ranging from 0.52 - 0.59 (Green), 2<sup>nd</sup> band is ranging from 0.62 -

0.68 (Red), 3<sup>rd</sup> band is ranging from 0.77 - 0.86 (Near Infra-red) and 4<sup>th</sup> band is ranging from 1.55 - 1.70 (Shortwave Infrared-red) with 23.5m resolution/ pixel.

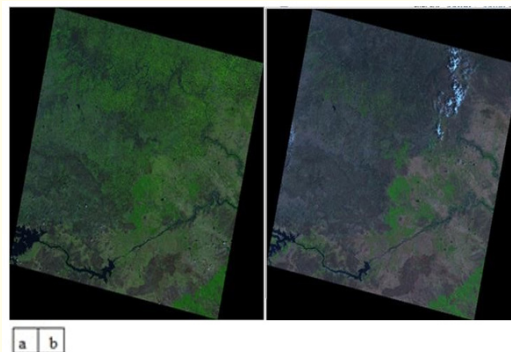


**Figure 1:** a. IRS-1C LISS III image dated 20th October 2006; b. IRS-1C LISS III image dated 11th April 2006.

### Methodology

Identification of geophysical topographies in a satellite image is a specific task since the spectral reflectance changes under different atmospheric conditions. Initially, before going to extract the vegetation feature of satellite image, all four different bands are stacked together to get the one RGB image [16]. Features are instantaneously perceivable visually [4]. A satellite image of any dimension and size MxN can be characterized as matrices of Red, Green, and Blue (R, G, and B) components for visual clarity [17]. The resulting in 3 N dimensional vectors was adequate for analysis. The following flowchart in figure 2 represents the steps involved in proposed analysis method.

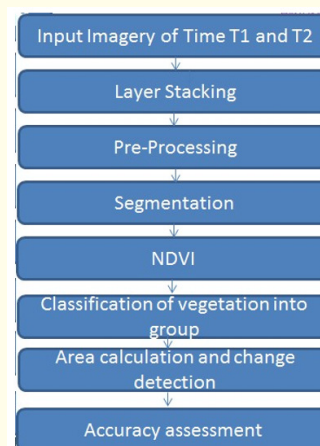


**Figure 2:** Flow Chart of the proposed Scheme.

Due to computational complexity and visual clarity of the data, given each frame was divided into 16 expedient blocks in MATLAB. Smaller frames of sufficient geo-spatial information were taken. A sub frame size of 700\*700 pixels contains a significant measure of geo-spatial information. Block 11 was taken for the analysis because of existence of variety of land cover.

**Pre-processing**

The two, geometrically co-registered IRS C LISS III imagery belonging to study area was obtained for this research. Filtering operation often affects clean pixels as well, resulting in overall blurring including edges and reduction of overall quality of the image [18,19]. PDE can be used to automatically produce an image of enhanced quality, with noise filtered and maintained shapes and edges. Images will have high correlation with neighboring pixels with probably similar values for similar texture. The similarity between the different band of the study image was employed [20]. Noise free image band with high signal to noise ratio was used as priors in enhancement process. Auxiliary image was introduced as reference image or base image into PDE in enhancement process. An image  $I(x, y)$  represents the pixel with relative intensity values at  $(x, y)$  location, basic features of the image such as "edges," gradients were given by  $I = (I_x, I_y)$ .  $I_x$  is partial derivative of  $I$  with respect to  $x$ ,

$I_y$  is the partial derivatives of  $I$  with respect to  $y$ . Gradient operator was given by formula 1,

$$\nabla = \left( \frac{\partial}{\partial x}, \frac{\partial}{\partial y} \right) \dots\dots\dots (1)$$

Total variation de-noising model is given by

$$TV(I) = \int_S |\nabla I| dx dy + \frac{\lambda}{2} \int_S (I - I_0)^2 dx dy. \dots\dots\dots (2)$$

Where the support area of the image is  $s$ , regularization term, gives the regularization parameter and was the modulus of gradients of  $I$ . Similarity between the directions of the edges and correlation between the auxiliary image and the base image was used to conserve edge details and smooth out noise. Resulting image was subjected histogram equalization [8,21], for visible clarity. Histogram Equalization spreads out the gray intensity levels of the image to reach white, resulting in increased dynamic range of gray levels and consequently increases in image contrast. PDE enhanced image and histogram equalized image relating to IRS1C LISS III im-

age dated 20th October 2006 pre-processed image, can be seen in figure 3.

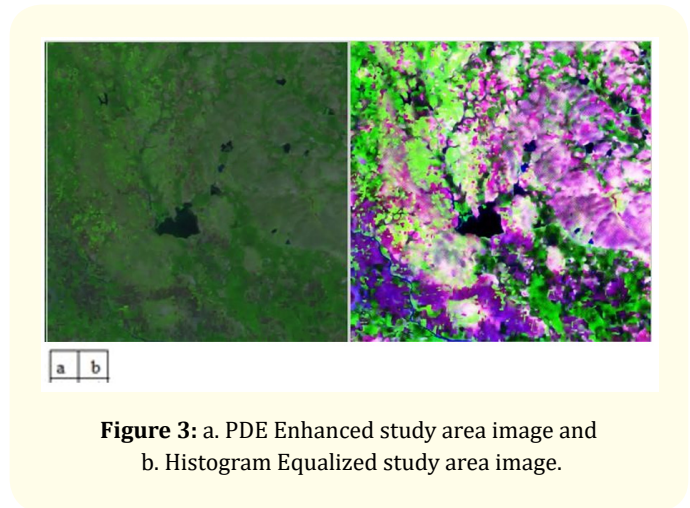


**Figure 3:** a. PDE Enhanced study area image and b. Histogram Equalized study area image.

**Segmentation**

The selection of segmentation approach depends on what quality of segmentation is required and on what is the scale of information required, for land use coarse scale segmentation is required whereas for land cover fine scale [22]. Level set method is an active contour based model. The method uses an active curve objective functional with two terms: an original term which evaluates the deviation of the mapped image data within each segmentation region from the piecewise constant model and a classic length regularization term for smooth region boundaries [9,23]. Level set method implements a systematic general mapping between the segmentation regions and the regions defined by the curves and their intersections [24]. Homogeneity measure based on texture segmentation inherits spectral and spatial properties in itself. Gray Level Co-occurrence Matrices (GLCM) is a statistical method. It describes the image pixel's gray scale distribution and structural features from various aspects [25]. GLCM measures frequency of occurrence of different combinations of pixel brightness values. Because typically two samples are compared [10]. For image  $I(x, y)$ : Energy, Entropy, Contrast, Variance, Homogeneity and Correlation are the various parameters which are calculated by using following formulas.

$$\text{Energy, } E = \sum_{x=1}^M \sum_{y=1}^N I(x, y)^2 \dots\dots\dots (3)$$

$$\text{Entropy, } E_n = - \sum_{x=1}^M \sum_{y=1}^N I \log_2 I(x, y) \dots\dots\dots (4)$$

$$\text{Contrast, } C = \sum_{x=1}^M \sum_{y=1}^N (x - y)^2 I(x, y) \dots\dots\dots (5)$$

Where  $\mu$  is the mean

$$\text{Variance, } V = \sum_{x=1}^M \sum_{y=1}^N (x - \mu)^2 I(x, y) \quad \dots\dots (6)$$

$$\text{Homogeneity, } H = \sum_{x=1}^M \sum_{y=1}^N \frac{1}{1+(x,y)^2} I(x, y) \quad \dots\dots (7)$$

$$\text{Correlation, } Co = \frac{\sum_{x=1}^M \sum_{y=1}^N (x,y)I(x,y) - \mu_x \mu_y}{\sigma_x \sigma_y} \quad \dots\dots (8)$$

Where  $\mu_x, \mu_y$  and  $\sigma_x, \sigma_y$ , are the mean and standard deviations

These features are stored in the feature library. Based on the GLCM parameters similar texture pixels are clustered into segments. Statistical segmentation algorithm requires initialization of number of segmentation classes and iterative procedure [6] of segmentation, based on the current parameters. Four broader classes namely, water bodies, Uncultivated open lands and settlements, barren lands and vegetation, were separated out based on the pixel reflectance ranges. The figure 4 depicts the vegetation feature from the study block.

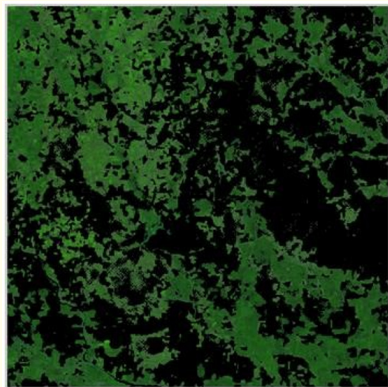


Figure 4: Vegetation Extracted image.

There were totally 491401 number of pixels. Total 232459 pixels are vegetation pixels. Percentage of vegetation occupancy in the block was calculated by using the formula 9.

$$\text{Percentage of vegetation } (\%) = \left[ \sum_{x=1}^M \sum_{y=1}^N \frac{I(x,y)}{T(x,y)} \right] * 100 \quad \dots\dots (9)$$

percentage of the block depicts vegetation.

**Classification**

Spectral brightness and geo-spatial characteristics in an satellite image were used for classification by dividing pixels into different categories [25]. The principal objective of the proposed method was vegetation extraction followed by vegetation classification. Very difficult part of the classification is to decide the appropriate

characteristics based on that the classifier is going to classify the different classes from each other [16]. Removal of non-vegetation pixels enables classification algorithm to differentiate among different vegetation types. Euclidean distance represents images as points in a high dimensional image space. If  $I = (I_1, I_2, \dots, I_{mn})$  and  $J = (J_1, J_2, \dots, J_{mn})$  are the two images of size  $M*N$ .  $I_k; J_k$  are gray levels on  $K^{th}$  pixels, the Euclidean distance [12],  $d_E^2(I, J)$  is given by formula 9.

$$d_E^2(I, J) = \sum_{K=1}^{MN} (I^K - J^K)^2 \quad \dots\dots (9)$$

The pair with more similarity has a larger Euclidean distance. Each pixel from the study image can be classified by calculating the Euclidean distance between given pixel and reference pixel. Class 4 and the Class 3 show significant variations, this helps for vegetation discrimination. The classified results are shown in figure 5. Color differencing is used to identify each pixel with different reflectance.

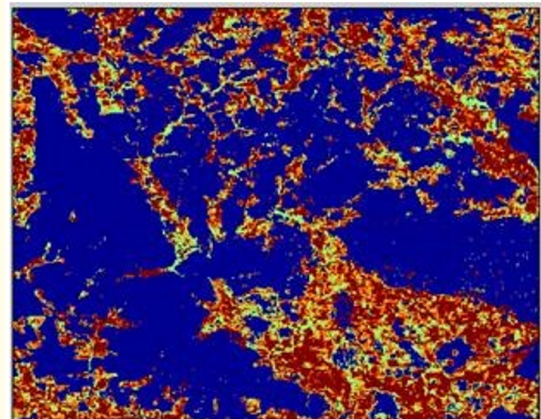


Figure 5: Classified image.

There could be four possible classes. Each color in classified image represents a particular class of vegetation. These segmented pixels were separated to generate individual class image. Dark blue color depicts masked region, brown depicts class 3, Yellow color depicts class 2 and light green color depicts class 4 covered areas and white color depicts class 1. Resulting, four spatially separated images of 11th April 2006 (T1 image) were shown in figure 8.

**Results**

**Performance evaluation**

Statistical quantitative analysis was done to evaluate the performance evaluation of the proposed algorithm. Statistical accuracy

was determined by computing error or confusion matrix of the proposed classification, with overall accuracy indicators. The confusion or error matrix was generated from known vegetation patterns used for training (columns) versus the pixels actually classified into each land cover classes by classifier (rows). As the focus of the study is vegetation, only vegetation features were extracted by NDVI, it is the best indicator for seasonal changes and vegetation cover [26,27]. Spectral pixel values of the study image along with the NDVI calculated were used for initial classification [28]. NDVI was calculated by using near-infrared band (NIR) and red band (RED) band reflectance values. NDVI formula was shown below.

$$NDVI = (NIR - RED) / (NIR + RED) \quad (10)$$

The NDVI is a non-dimensional values ranging from -1.0 and +1.0. NDVI of dense vegetation will range from 0.3 to 0.5 [28,29].

Predefined thresholds were chosen that are relevant for the classification. Resultant image pixels were divided into four groups. Table 1 shown below is generated with row values corresponding to classes in the NDVI segmented image data taken as class type determined by the reference source. Column values were generated by the classes of proposed classification. Correctly classified pixels of each class were tabulated diagonally in table 1. Off-diagonal column elements represent actual pixels of other classes that were wrongly included in a certain classification class. The algorithm was used for multitemporal geometrically registered images. Image acquired on 11<sup>th</sup> April 2006 was considered as T1 image and Image acquired on 28<sup>th</sup> October 2006 was considered as T2 image, for the analysis. Confusion matrix with accuracy estimate was shown in table 1 for T1 image and table 2 for T2 image.

		Class type determined by the reference source						
Classes		Class 1	Class 2	Class 3	Class 4	Total pixels	User`s Accuracy	
Class type determined from classified map	Class 1	4	0	0	0	4	100.0	Over all accuracy is 83.21%
	Class 2	0	932	0	97	1029	90.6	
	Class 3	0	107 58	64762	0	75520	85.8	
	Class 4	0	0	35860	466 27	82487	56.5	
	Total	4	116 90	1006 22	467 24	159040	332.9	
Producer`sAccuracy		100.0	8.0	64.4	99.8	272. 1	70.6	
		Over all Producer`s accuracy is 68.03%					Over all accuracy for T1 image is 71.6%	

Table 1: Confusion Matrix for Image T1.

		Class type determined by the reference source						
Classes		Class 1	Class 2	Class 3	Class 4	Total pixel s	User`s Accuracy	
Class type determined from classified map	Class 1	476	0	0	0	476	100.0	Over all accuracy is 81.89%
	Class 2	0	6415	0	1427	7842	81.8	
	Class 3	0	26412	66338	0	92750	71.5	
	Class 4	0	0	33822	975 69	1313 91	74.3	
	Total	476	32827	1001 60	98996	232459	327.6	
Producer`s Accuracy		100	20	66	99	284	73.5	
		Over all Producer`s accuracy is 71.00%					Over all accuracy T2 image is 73.5%	

Table 2: Confusion matrix for Image T2.

Resulting graph of relative user`s and producer`s accuracy for T1 image and T2 image was demonstrated in figure 6 and figure 7 correspondingly.

In figure 6 class 1, class 3 and class 4 user`s accuracy was better, but for class 2 user`s accuracy has dropped. Because of which, resultant average 83% user`s accuracy and 68% producer`s accuracy was obtained for T1 image.

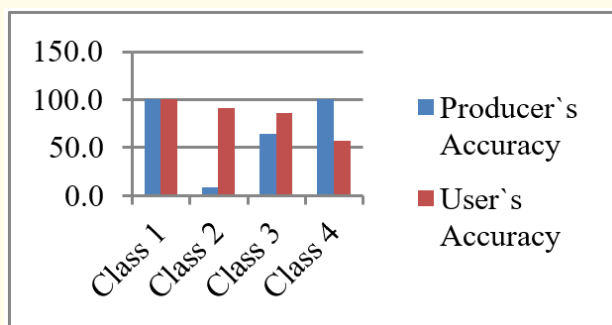


Figure 6: Graph of User's v/s Producer's accuracy for T1 image.

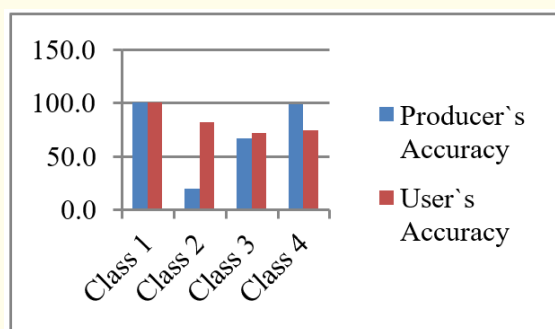


Figure 7: Graph of User's v/s Producer's accuracy for T2 image.

Resulting graph of relative user's and producer's accuracy for T2 image was demonstrated in figure 7.

For three classes like class 1, class 3 and class 4 user's accuracy was better, but for class 2 user's accuracy has dropped. Resultant average 81% user's accuracy and 71% producer's accuracy was obtained for image T2. The column statistics of Table 1 and Table 2 contribute for over all producer's accuracy. This presents the accuracy of proposed classification, measures the errors of omission (1 - producer's accuracy). Producer's accuracy for T1 and T2 are 68% and 71%. The figures in row of Table 2 and Table 3 contribute User's accuracy (Reliability) present the reliability of classes in the classified image, measures the error of commission (1- use's accuracy). User's accuracy for T1 and T2 are 83% and 81%. Over all accuracy was represented by diagonal representing pixels correctly classified with respect to reference data. Over all accuracy of proposed classification for T1 and T2 imagery were 71% and 73% respectively.

Cohen's Kappa co-efficient calculates the dissimilarity between actual agreement and the agreement expected by chance [30] as shown in formula 11. Observed accuracy was determined by diago-

nal values in confusion matrix. Chance agreement was measured by off diagonal values.

$$Kappa = \frac{\text{(observed accuracy - chance agreement)}}{(1 - \text{Chance agreement})} \dots\dots (11)$$

From the results, Kappa coefficient for T1 is 0.9968 means there is 99.68% better agreement than by chance alone. Kappa coefficient for T2 is 0.9969 means there is 99.69% better agreement than by chance alone.

**Change detection**

Data acquired by the same satellite sensor of same spatial, spectral and radiometric resolution was used for change detection analysis. Data acquired at unchanged viewing angles but multi-temporal [31] images was required to characterize the environmental changes of vegetation. Discriminate among hierarchical vegetation cover, with similar spectral response, was possible by the proposed algorithm. Proposed algorithm was repeatedly executed to discriminate clearly between different classes of vegetation and for consistent handling of the data. The multi-temporal statistics of these classes, as shown in table 3, gives spatio-temporal pixel differences of the vegetation. This improves the separation of vegetation patterns. Four spatially separated images of 11<sup>th</sup> April 2006 (T1 image) were shown in figure 8.

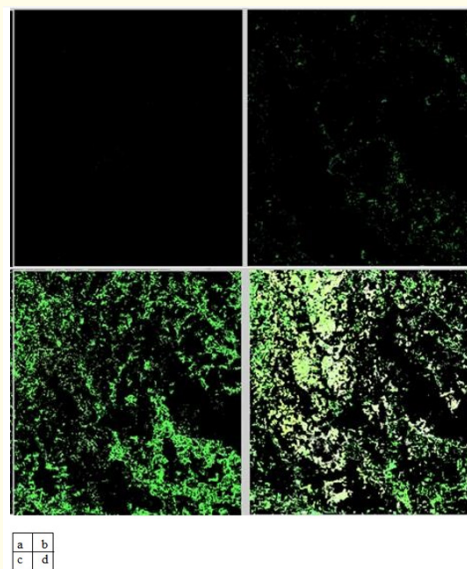
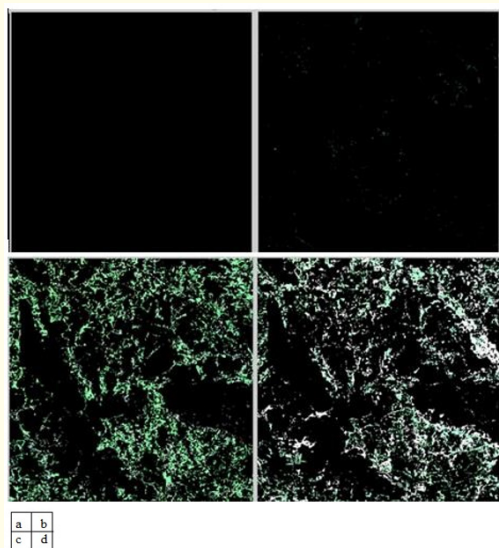


Figure 8: Vegetation extracted image was hierarchal segmented into four classes for T1 image; a. Class 1 image, b. Class 2 image, c. Class 3 image and d. Class 4 image.

Vegetation pixels in T1 image were 159040, with 47.30% occupancy. Similarly, image dated 28th October 2006 (T2) was clas-

sified by proposed algorithm. Resulting four images were shown in figure 9.



**Figure 9:** Vegetation extracted image was hierarchical segmented into four classes for T2 image. a. Class 1 image, b. Class 2 image, c. Class 3 image and d. Class 4 image.

Vegetation pixels in T2 image were 159040 pixels with 32.3% occupancy. There was an increase of 73419 pixels in classified image dated T2 with respect to classified image dated T1, due to temporal environmental differences. As a result, 14.94% increase in overall vegetation cover, was observed in T2 image.

Further, as vegetation was classified into four classes (table 3); it is possible to determine changes in hierarchical vegetation patterns. It was observed, from the statistical change analysis, that all three classes of classification demonstrations declined vegetation cover excluding class 3. Positive percentage indicates increase in the agricultural area. The upsurge in the agricultural area was due to periodic changes in the environment. These statistical changes were tabulated in Table 3.

The accuracy of proposed algorithm for change detection in vegetation cover can be better tested with of more number of multitemporal images with optimal acquisition dates [28,32]. Figure 10 exhibits graphical representation of vegetation classes.

Increase in the growth of class 3 was observed followed by decrease in remaining classes.

Classes	Number of classified pixels for T1 Image	Percentage area of occupancy of different classes	Number of classified pixels for T2 Image	Percentage area of occupancy of different classes	Percentage Change Detected
Class 1	1.0	0.0	139.0	0.1	-0.1
Class 2	1032.0	0.6	8179.0	3.5	-2.9
Class 3	75520.0	47.5	92750.0	39.9	7.6
Class 4	82487.0	51.9	131391.0	56.5	-4.7

**Table 3:** Statistical Change Detection.

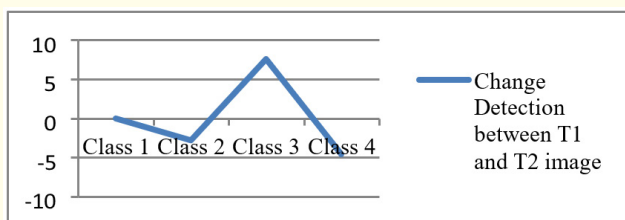


**Figure 10:** Percentage change observed.

**Conclusion**

Vegetation discrimination enables the user to identify the hierarchy available in the vegetation cover automatically, by masking non vegetation features. The proposed algorithm was repeated for

multitemporal IRS-1C LISS III images. Visually clearer results were obtained by applying PDE based enhancement. Multiphase Level set segmentation gives systematic general mapping between the segmentation region, thus separating land cover features. Statistics of GLCM were analyzed accurate for feature extraction. Finally, vegetation patterns were classified into various classes. Difference between proposed method of classification and reference data was evaluated for accuracy assessment. The accuracy assessment reflects authentication of the proposed algorithm, with respect to reference data. Over all accuracy for two multi-temporal images was 71% and 73% respectively. Cohen's kappa coefficient was generated for numerical evaluation of better inter-rater agreement. Kappa coefficient was 0.99.demonstrating 99% better agreement by chance. This work was extended for change detection for track-

ing the phenological vegetation changes. Hierarchical class wise change in overall vegetation cover was observed between multi-temporal study areas. Percentage changes related to every class was also tabulated. This work can be extended for extraction of cultivated and barren land identification, with emphasis on land fertility analysis. The assessment of the proposed study was restricted because of accessibility of a minimum number of images of different acquisition dates images.

### Acknowledgment

The authors would like to thank Karnataka State Remote Sensing Centre, Regional Office, Kalaburagi, Karnataka, India, for sharing IRS-1C LISS III images for the study. The authors praise their competence and willingness to help.

### Bibliography

1. KK Ahsan Ahmad., *et al.* "Fusion of Textural and Spectral Information for Tree Crop and Other Agricultural Cover Mapping with Very-High Resolution Satellite Images". *IEEE Journal of selected topics in applied Earth observations and Remote Sensing* 5.1 (2012): 225-235.
2. BKS Pavan Kumar., *et al.* "An Efficient Hybrid Classification Approach for Land Use/Land Cover Analysis in a Semi-Desert Area Using ETM+ and LISS-III Sensor". *IEEE Sensors Journal* 13.6 (2013): 2161-2165.
3. SR Pudale and UV Bhosle. "Comparative Study of Relative Radiometric Normalization Techniques for Resourcesat1 LISS III Sensor Images". *IEEE Computer Society* 8 (2007): 233-239.
4. Verma., *et al.* "Development of Descriptors for Natural Feature Identification on IRS LISS III Images". *Methods and Models in Computer Science (ICM2CS), International Conference 4* (2010): 54-58.
5. Bo Chen., *et al.* "A Multiplicative Noise Removal Approach Based on Partial Differential Equation Model". *Mathematical Problems in Engineering* 1 (2012): 2-14.
6. A Rekik., *et al.* "A kMeans Clustering Algorithm Initialization for Unsupervised Statistical Satellite Image Segmentation". *E Learning in Industrial Electronics*, 1ST IEEE International Conference 3 (2006): 11-16.
7. RB Inampudi., *et al.* "Knowledge Based Approach for Automated Digital Image Processing". *IEEE conference on Geoscience and Remote Sensing Symposium* (2002): 1340-1342.
8. SV Bharathi S., *et al.* "Performance Analysis of Segmentation Techniques for Land Cover Types using Remote sensing image". *India Conference (INDICON), Annual IEEE* (2012): 775-780.
9. AM Mohamed Ben Salah., *et al.* "Effective Level Set Image Segmentation With a Kernel Induced Data Term". *IEEE Transactions on Image Processing* 19 (2010): 220-232.
10. JD Christoph Georg Eichkitz., *et al.* "Grey level co-occurrence matrix and its application to seismic data". *Special Topics on Modelling/Interpretation* 33 (2015): 71-77.
11. XC Genyun Sun., *et al.* "Combinational Build-Up Index (CBI) for Effective Impervious Surface Mapping in Urban Areas". *IEEE Journal of selected Topics in applied Earth Observation and Remote sensing* 99 (2012): 1-12.
12. YZ Liwei Wangy, Jufu Fengy. On the Euclidean Distance of Images.
13. DS Ana Carolina Siravenha., *et al.* "Atmospheric components: analyzing inpainting methods to removal these occurrences in remote sensing images". *International Journal of Signal Processing, Image Processing and Pattern Recognition* 5.2 (2012): 22-46.
14. P Ravindra., *et al.* "Hybrid Image Classification Technique for Spatio-temporal Analysis of Pune City". *Trans. Inst. Indian Geographers* 35.2 (2013): 213-223.
15. District administration. Geographical Features and Socio Economic and Cultural Characteristic of Yadgir District.
16. K Anand Upadhyay and Thakur Village. "Classification of IRS LISS-III Images Using PNN". *Computing for Sustainable Global Development (INDIACom), 2nd International Conference* 8 (2015): 416-420.
17. DN Verma., *et al.* "Development of Descriptors for Natural Feature Identification on IRS LISS III Images". *Methods and Models in Computer Science (ICM2CS), International Conference 4* (2010): 54-58.
18. P Ravi., *et al.* "A Novel PDE Based Diffusion Technique for Image Denoising". *International Journal of Advanced Electrical and Electronics Engineering* 2.1 (2013): 52-51.
19. FMaH. Ghassemian. "Hyperspectral Image Classification using profiles based on Partial Differential Equations". *Presented at the 23rd Iranian Conference on Electrical Engineering Iran* (2015): 288-292.
20. FH Peng Liu., *et al.* "RemoteSensing Image Denoising Using Partial Differential Equations and Auxiliary Images as Priors". *IEEE Geoscience and Remote Sensing Letters* 9.3 (2012): 358-362.
21. NSP Kong and H Ibrahim. "Color Image Enhancement Using Brightness Preserving Dynamic Histogram Equalization". *IEEE Transactions on Consumer Electronics* 54.4 (2008): 1962-1968.

22. V Dey. "A Review on Image Segmentation Techniques with Remote Sensing Perspective". *ISPRS TC VII Symposium* 38 (2010): 31-42.
23. TC Luminta Vese. "A Multiphase Level Set Framework for Image Segmentation Using the Mumford and Shah Model". *International Journal of Computer Vision* 50.3 (2002): 271-293.
24. AM Abdol-Reza Mansouri, *et al.* "Multiregion competition: A level set extension of region competition to multiple region image partitioning". *Computer vision and image understanding* 101.3 (2005): 137-150.
25. WZ Jianhong Liu, *et al.* "Cropland Parcels Extraction Based on Texture Analysis and Multi- spectral Image Classification". 2010.
26. YW Feng Zhang and Ying Li. "Land Cover Information Extraction Based on Multi-Temporal HJ-1 Satellite Images". *IEEE International Geoscience and Remote Sensing Symposium* 5.3 (2012): 4962-4965.
27. WJP Dao-li. "A research on extracting information of the arid regions vegetation coverage using improved model of spectral mixture analysis". *Multimedia Technology (ICMT), International Conference* 3 (2010): 1-5.
28. AG Erik Zillmann, *et al.* "Pan-European Grassland Mapping Using Seasonal Statistics From Multisensor Image Time Series". *IEEE Journal of selected of topics in applied in applied Earth Observations and Remote Sensing* 7.8 (2014): 3461-3472.
29. HY Ali Mermeri, *et al.* "Monitoring Rangeland Vegetation Through Time Series Satellite Images (NDVI) In Central Anatolia Region". *4th Interntion confrence on Agro Informatics* (2015): 213-216.
30. EAMH Abubaker Haroun Mohamed Adam, *et al.* "Accuracy Assessment of Land Use and Land Cover Classification (LU/LC) –Case study of Shomadi area -Renk County-Upper Nile State, South Sudan". *International Journal of Scientific and Research Publications* 3.5 (2013): 1-5.
31. S Singh and R Talwar, "A Quantitative Analysis of Different Change Detection Algorithms over Rugged Terrain MODIS Sensor Satellite Imagery". *Signal Processing and Communication (ICSC), International Conference* 2 (2015): 273-278.
32. HW Erik Zillmann, *et al.* "Mapping of grassland using seasonal statistics derived from multi-temporal satellite images". *Research Gate* (2013): 1-4.

**Volume 3 Issue 4 April 2019**

© All rights are reserved by Rubina Parveen, *et al.*